Article

Cell Reports

Effector and Regulatory T Cells Roll at High Shear Stress by Inducible Tether and Sling Formation

Graphical Abstract

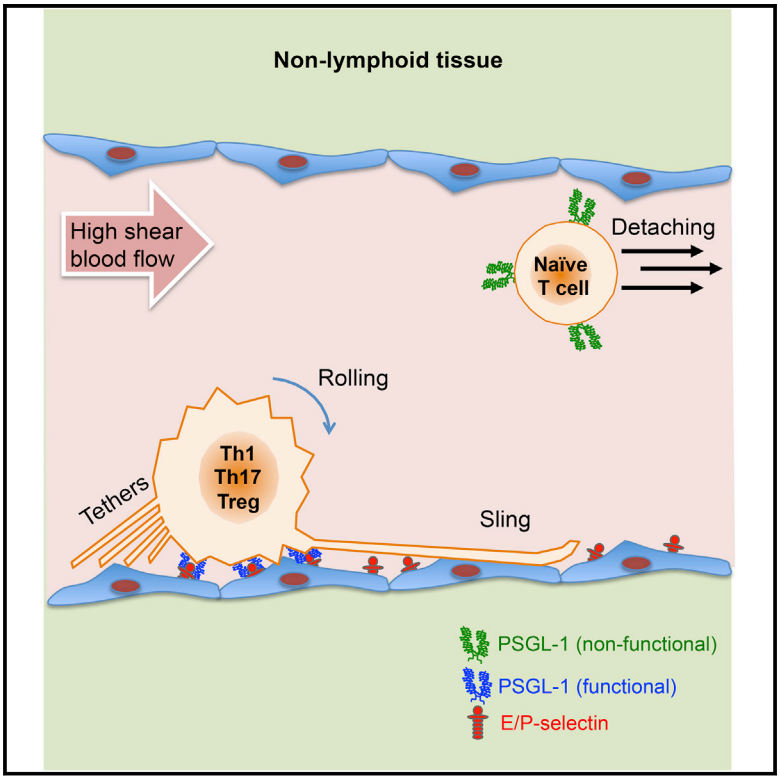

Authors

Michael Abadier, Akula Bala Pramod, Sara McArdle, ..., Edgar Gutierrez, Alex Groisman, Klaus Ley

Correspondence

klaus@lji.org

In Brief

Abadier et al. report that profound transcriptomic changes during CD4 T cell differentiation enable effector and regulatory T cells to form tethers and slings, enabling rolling at high shear stress. This inducible phenotype facilitates Th1, Th17, and Treg cell rolling and homing to inflamed peripheral tissues.

Highlights

- Tethers and slings are inducible in mouse and human differentiated CD4 T cell subsets
- Th1, Th17, and Treg cells but few Th2 cells bind selectins and induce tethers and slings
- The sling-forming T cells show overexpression of genes controlling cell migration
- Tethers and slings allow Th1, Th17, and Treg cells to infiltrate non-lymphoid tissues

Data and Software Availability

GSE107981

Abadier et al., 2017, Cell Reports *21*, 3885–3899
December 26, 2017
https://doi.org/10.1016/j.celrep.2017.11.099

CellPress

Cell Reports
Article

Effector and Regulatory T Cells Roll at High Shear Stress by Inducible Tether and Sling Formation

Michael Abadier,[1] Akula Bala Pramod,[1] Sara McArdle,[1] Alex Marki,[1] Zhichao Fan,[1] Edgar Gutierrez,[2] Alex Groisman,[2] and Klaus Ley[1,3,4,*]
[1]Division of Inflammation Biology, La Jolla Institute for Allergy and Immunology, La Jolla, CA 92037, USA
[2]Department of Physics, University of California San Diego, La Jolla, CA 92093, USA
[3]Department of Bioengineering, University of California San Diego, La Jolla, CA 92093, USA
[4]Lead Contact
*Correspondence: klaus@lji.org
https://doi.org/10.1016/j.celrep.2017.11.099

SUMMARY

The adaptive immune response involves T cell differentiation and migration to sites of inflammation. T cell trafficking is initiated by rolling on inflamed endothelium. Tethers and slings, discovered in neutrophils, facilitate cell rolling at high shear stress. Here, we demonstrate that the ability to form tethers and slings during rolling is highly inducible in T helper 1 (Th1), Th17, and regulatory T (Treg) cells but less in Th2 cells. *In vivo*, endogenous Treg cells rolled stably in cremaster venules at physiological shear stress. Quantitative dynamic footprinting nanoscopy of Th1, Th17, and Treg cells uncovered the formation of multiple tethers per cell. Human Th1 cells also showed tethers and slings. RNA sequencing (RNA-seq) revealed the induction of cell migration and cytoskeletal genes in sling-forming cells. We conclude that differentiated CD4 T cells stabilize rolling by inducible tether and sling formation. These phenotypic changes approximate the adhesion phenotype of neutrophils and support CD4 T cell access to sites of inflammation.

INTRODUCTION

Naive T (Tn) cells continuously recirculate between blood and specialized lymphoid organs, but effector and regulatory T cells must traffic to non-lymphoid sites to function. Upon antigen encounter and co-stimulation, naive CD4 T cells proliferate and differentiate to various T cell lineages, including T helper 1 (Th1), Th2, Th17, and regulatory T (Treg) cells. T cells commit to Th1 cells in the presence of interleukin (IL)-12; Th2 cells in the presence of IL-4, IL-5, and IL-13; Th17 cells in the presence of IL-1, transforming growth factor beta (TGF-β), IL-6, and IL-21; and Treg cells in the presence of TGF-β and IL-2 (Zhu et al., 2010).

The initial step of effector or regulatory T cell trafficking is dependent on selectins (P- or E-selectin) binding to their highly glycosylated carbohydrate ligand PSGL-1, which controls the transient interaction between T cells flowing in the bloodstream at high shear stress and the inflamed blood vessel wall in a process known as tethering and rolling (Fu et al., 2016). It is known that PSGL-1 expression does not directly correlate with its ability to bind selectins (Abadier and Ley, 2017; Ley and Kansas, 2004). Neutrophils constitutively express enzymes required for PSGL-1 glycosylation, but PSGL-1 on Tn cells fails to bind P-selectin. Several posttranslational modifications are required for functional PSGL-1 biosynthesis. These enzymatic modifications include sialylation by at least two sialyl transferases (one of them is St3gal-IV, *St3gal4* gene), fucosylation by α1,3-fucosyltransferases (FucT-IV, *Fut4* gene; FucT-VII, *Fut7* gene), tyrosine sulfation by at least one of the two tyrosine sulfotransferases (*Tpst1* or *Tpst2* gene), and generation of branched carbohydrate side chains by the core 2 glycosyl transferase (C2GlcNAcT-I, *Gcnt1* gene) (Sperandio et al., 2009). PSGL-1 has one P-selectin binding site near its N terminus and multiple E-selectin binding sites located in O-glycan repeats (McEver and Cummings, 1997). Cytokine stimulation during antigen presentation and T cell differentiation shapes transcriptional activity, which has a direct influence on the synthesis of glycosyl transferases (Hobbs and Nolz, 2017). Th1 cells are known to have highly functional PSGL-1, which explains the enhanced binding of Th1 cells to P- or E-selectin compared with Th2 cells (Austrup et al., 1997; Borges et al., 1997b). At the time of these studies, tethers, slings, Th17, and Treg cells had not yet been discovered.

Selectin binding is essential to mediate stable leukocyte rolling, which is characterized by consistently low rolling velocity with little variation and low rates of detachment (Zarbock et al., 2011). At high shear stress (>6 dyn/cm^2), once pulling forces exceed a critical threshold of ~35 pN per microvillus (Pospieszalska et al., 2011), tethers and slings form and stabilize cell rolling (Sundd et al., 2012). Tethers are formed from pre-existing leukocyte microvilli and can reach lengths of 30 μm. When tethers detach and swing around the rolling cell, they can become slings, self-adhesive substrates initially discovered in neutrophils (Sundd et al., 2012). All tether and sling work so far has been conducted in neutrophils. Naive CD4 T cells cannot make either tethers or slings at high shear stress. Here, we systematically investigated how CD4 T cell differentiation affects tether and sling formation.

Tn cells use L-selectin to roll on peripheral node addressins (PNAd) and arrest when CCL21 binds CCR7 (von Andrian and Mackay, 2000). The L-selectin-PNAd interaction is restricted to high endothelial venules, where wall shear stress is ~1 dyn/cm^2 (Lawrence et al., 1997; Dixon et al., 2006). After Tn cells encounter their cognate antigen, they differentiate and acquire receptors for homing to inflammatory sites within non-lymphoid organs (Krummel et al., 2016; Ley, 2014). T cell recruitment during inflammation or infection occurs mostly in postcapillary venules, where the wall shear stress exceeds 6 dyn/cm^2 (Ley and Gaehtgens, 1991). Thus, we hypothesized that differentiated T cells undergo transcriptional reprogramming enabling tether and sling formation to effectively roll, slow down, and transmigrate at sites of inflammation.

Here we report that PSGL-1 is not functional in Tn cells but gains moderate functionality in Th2 cells and full functionality in Th1, Th17, and Treg cells. This is mirrored by elevated expression of *Gcnt1*, *Fut4*, and *Fut7*, which are required for PSGL-1 glycosylation. As a consequence, Th1, Th17, and Treg cells show stable rolling on P- or E-selectin. Th2 cells showed faster, unstable rolling with more detaching cells. Most Th1, Th17, and Treg cells formed about seven or eight tethers per cell, while Th2 cells formed fewer than five tethers per cell. *In vivo*, endogenous Tregs rolled efficiently in cremaster vessels of Foxp3-YFP mice at physiological shear stress. All CD4 T cells that form slings underwent similar transcriptional changes that induced common pathways related to cell migration and cytoskeleton organization. To translate these findings, we studied primary human Th1 cells sorted from blood and found that they also form tethers and slings and, like mouse CD4 T cells, can roll on P-selectin. Collectively, our data explain the excellent rolling behavior of Th1, Th17, and Treg cells, which acquire transcriptomes closer to that of neutrophils and readily form tethers and slings.

RESULTS

P-Selectin Binding Is Enhanced in Differentiated CD4 T Cells

We differentiated mouse Tn cells (CD62L^{hi}CD44^{lo}) to Th1, Th2, Th17, or Treg cells for 72 hr *in vitro* (Figure S1A). First, we confirmed the polarization of mouse T cells into distinct subsets by measuring their cytokine production and transcription factors. High expression of the cognate signature cytokines and transcription factors was observed by flow cytometry and transcriptomics for interferon (IFN)-γ and T-bet (Tbx21) in Th1 cells; IL-4 and Gata-3 in Th2; IL-17A, IL-17F, ROR-γt (Rorc), and Rora in Th17 cells; and Foxp3 in Treg cells (Figures S1B and S1C).

To elucidate PSGL-1 functionality in the CD4 T cell subsets, we measured P-selectin-Fc dimer binding using flow cytometry. Neutrophils (which bind P-selectin) and Tn cells (which do not bind P-selectin) were used as positive and negative controls, respectively (Figure S2A). The surface-expressed PSGL-1 protein level was similar in neutrophils, Tn, Th1, Th2, Th17, and Treg cells (Figures S2B and S2C). As expected, most neutrophils (76 ± 2%) and very few Tn cells (4 ± 0%) bound P-selectin-Fc (Figures S2D and S2E). CD4 T cell differentiation led to higher percentages of P-selectin-Fc binding under Th1 (51 ± 4%)-, Th17 (57 ± 6%)-, and Treg (56 ± 5%)-inducing conditions than under Th2-inducing conditions (25 ± 4%) (Figure S2E).

PSGL-1 requires posttranslational modifications to be functional and successfully bind selectins (Figure S2F). To compare the enzymatic machinery involved in PSGL-1 functionality, we completed genome-wide sequencing (RNA sequencing [RNA-seq]) from Tn, Th1, Th2, Th17, and Treg cells, neutrophils, and promyelocytes. The seven cell types were isolated, differentiated *in vitro*, phenotyped by flow cytometry, and sorted using fluorescence-activated cell sorting (FACS) to >99% purity, generating enough cells to get high-quality RNA-seq data from three biological replicates (Figure S3 and Table S1). Specific markers for neutrophils and promyelocytes (Perera et al., 2013; Theilgaard-Mönch et al., 2005) were confirmed by transcriptomics (Figure S4). As expected, neutrophils and promyelocytes clustered together in the principal-component analysis (PCA) but were completely segregated from all types of CD4 T cells (naive or differentiated) (Figure S5A). A separate PCA plot for only CD4 T cells showed a clear segregation of naive from all differentiated T cells in PC1 (Figure S5B).

To explain the high binding capacity of Th1, Th17, and Treg cells to P-selectin-Fc (Figure S2E), we compared the expression of genes important for PSGL-1 functionality with neutrophils or promyelocytes (positive controls), Tn (negative control), and Th2 cells (Figures S2G and S6A). The core 2 acetylglucosaminetransferase C2GlcNAcT-I (*Gcnt1*) and fucosyltransferase FucT-VII (*Fut7*) were elevated in Th1, Th17, and Treg cells but nearly absent in Tn cells and only slightly induced in Th2 cells (Figures S2G and S2H). Notably, FucT-IV (*Fut4*) was upregulated in Th1 and Th17 cells but significantly higher in Treg cells. However, in all T cell subsets, *Fut4* did not reach the level seen in neutrophils or promyelocytes (Figure S6A). As expected (Blander et al., 1999), the sialyl transferase *St3gal4* was very low in Tn cells but was expressed at comparable levels in all four CD4 T cell subsets (Figures S2G and S6B). Interestingly, the tyrosyl sulfotransferase *Tpst2* was constitutively expressed in Tn cells, whereas *Tpst1* was induced in all differentiated CD4 T cell subsets (Figure S2G). The β1,4-galactosyltransferase-I *B4galt1* was high in Th17 and Treg cells but low in Th1 cells (Figure S2G). Because Th1 cells bind P-selectin well (Figure S2E) but do not express much *B4galt1*, we conclude that glycan extension is probably not a limiting step for P-selectin binding. Also, we observed that the α2,6-sialyltransferases *St6galnac4* and *St6galnac6*, but not α2,3-sialyltransferase *St3gal4*, are induced at higher levels in Th1, Th17, and Treg cells that bind P-selectin well but not in Th2 cells that bind P-selectin poorly (Figure S6B).

Taken together with the known requirements for PSGL-1 functionality (Ley and Kansas, 2004; McEver, 2015), we think that the enhanced P-selectin binding in Th1, Th17, and Treg cells (Figure S2E) is probably due to the significant upregulation of *Gcnt1*, *Fut4* and *Fut7* that decorate PSGL-1 to facilitate selectin binding (Figure S2H).

Rolling at High Shear Stress Is Stabilized in Th1, Th17, and Treg Cells *In Vitro* and *In Vivo*

Rolling at high shear stress (>6 dyn/cm^2) requires not only functional selectin ligands but also cell deformation and the

Table 1. Analysis of Th1, Th2, Th17, and Treg Cell Rolling on P- or E-Selectin-Fc at 10 dyn/cm^2

	P-Selectin			E-Selectin		
	No. of Rollers	% of Detachment	Rolling Velocity	No. of Rollers	% of Detachment	Rolling Velocity
Th1	69 ± 7	21 ± 2	12.3 ± 0.4	56 ± 7	19 ± 8	2.5 ± 0.1
Th2	17 ± 4	64 ± 4	15.8 ± 0.8	14 ± 2	56 ± 9	2.3 ± 0.1
Th17	60 ± 6	14 ± 2	11.1 ± 0.3	64 ± 10	10 ± 2	1.7 ± 0.1
Treg	40 ± 5	26 ± 4	17.6 ± 0.7	45 ± 8	22 ± 4	2.3 ± 0.1

formation of tethers and slings (Sundd et al., 2013). This is well studied in neutrophils (Ramachandran et al., 2004; Sundd et al., 2012) but not in T cells. As expected, Tn cells did not bind (Figure S2E) or roll (data not shown) on P-selectin-Fc. To study the rolling behavior of the four differentiated CD4 T cell subsets, we allowed Th1, Th2, Th17, and Treg cells to settle in microfluidic flow chambers at 1 dyn/cm^2 on P-selectin-Fc and then increased the shear stress to 10 dyn/cm^2 (Table 1). Interestingly, large numbers of Th1, Th17, and Treg cells were able to roll at 10 dyn/cm^2, but the number of rolling Th2 cells was significantly smaller (Figure 1A). This rolling phenotype was mirrored by low rolling velocity (stable rolling) of Th1 and Th17 cells compared with Th2 cells (Figures 1B and 1C). Th2 cells showed a propensity to detach, whereas Th1, Th17, and Treg cells showed stable rolling (Figure 1D). Th1 and Th17 cells showed similar numbers of rolling cells, but Th17 cells rolled even slower than Th1 cells. This suggests a more stable rolling behavior of Th17 cells compared with Th1 cells.

Th1, Th17, and Treg cells also showed stable rolling on E-selectin-Fc (Figures 1E–1G and Table 1). The poor rolling of Th2 cells on E-selectin-Fc was mirrored by a much higher rate of detachment compared with Th1, Th17, and Treg cells (Figure 1H). Taken together, we found (1) enhanced ability to bind P-selectin (Figure S2E), (2) higher expression of crucial PSGL-1 glycosylation genes (Figure S2H), and (3) remarkably stable rolling (Figure 1; Table 1) of Th1, Th17, and Treg cells compared with Th2 cells.

To directly address the *in vivo* relevance of our findings, we performed intravital imaging in cremaster venules of Foxp3-YFP mice (Figure 2A; Movie S1). In these mice, endogenous Treg cells express YFP, which makes them visible by intravital microscopy without any experimental manipulations. YFP$^+$ Treg cells constitute ~13% of total CD4 T cells in blood of Foxp3-YFP mice (Figure 2B). Here, we used a model of acute inflammation in which surgical trauma-induced leukocyte rolling is mediated primarily by P-selectin (Pickard and Ley, 2009). The rolling of neutrophils (Ly6G$^+$) was used as positive control (Figure 2A, magenta). We found that Treg cells roll stably in cremaster postcapillary venules (Treg cells, 47 ± 4 μm/s; neutrophils, 28 ± 4 μm/s) (Figure 2C). This is consistent with our *in vitro* findings, in which neutrophils rolled at lower velocity than Treg cells on P-selectin-Fc at 10 dyn/cm^2 (Treg cells, 18 ± 1.0 μm/s; neutrophils, 6 ± 0.1 μm/s) (Figure 2D). Thus, Treg cells roll well, but not quite as well as neutrophils. This is also in line with substantial levels of *Gcnt1*, *Fut7*, and *Fut4* in *ex vivo* Treg cells isolated from Foxp3-GFP mice that are much higher than those in Tn cells (Figure S6C) (van der Veeken et al., 2016) but still lower than in neutrophils (Figure S6D).

Stably Rolling T Cells Form Tethers and Slings

Tethers and slings form in neutrophils rolling at high shear stress (>6 dyn/cm^2) (Sundd et al., 2012). To test whether differentiated Th1, Th2, Th17, and Treg cells acquire the ability to form tethers and slings, we used quantitative dynamic footprinting (qDF) nanoscopy, a technique that yields nanometer resolution in the vertical z axis (Sundd et al., 2010). We observed slings in all differentiated CD4 T cell subsets on P- and E-selectin-Fc (Figures 3A and 3B; Movies S2 and S3). Tethers are not directly visible on qDF, but the tether anchor points are visible (Sundd et al., 2010, 2012) (Figure 3C). Tether anchor points are absent at low shear stress (1 dyn/cm^2) but appear at 10 dyn/cm^2, and the numbers further increase with increasing shear stresses (Figure 3D). We found that the number of tether anchor points is inversely proportional to rolling velocity: a large number of tethers was associated with lower rolling velocity of T cells (Figure 3E). Th2 cells rolling on P- or E-selectin-Fc showed fewer tether anchor points than Th1, Th17, and Treg cells (Figures 3F and 3H). Most of the Th2 cells formed fewer than five tethers, whereas the average number of tethers in Th1, Th17, and Treg cells was about seven or eight tethers per cell (Figures 3G and 3I). Thus, the number of tether anchor points is large in slow-rolling cells (Th1, Th17, and Treg cells) and small in fast-rolling cells (Th2 cells) under the same conditions.

Tethers are thought to be formed from pre-existing cell microvilli (Sundd et al., 2012; Pospieszalska et al., 2011). We investigated the number of microvilli per rolling cell that touched the P- or E-selectin substrate. T cell footprints are the area of the cell that touches the substrate, which is visible by qDF (~0.2 μm). Interestingly, the number of microvilli in footprints of Th1 and Th17 cells was larger than Th2 cells on P-selectin-Fc (Figures 4A and 4C). Th2 cells rolling on E-selectin showed much fewer microvilli in contact with substrate than Th1, Th17, and Treg cells (Figures 4B and 4D).

RNA-Seq Analysis of Sling-Forming Cells Reveals a Transcriptomic Signature Related to Cell Migration and Cytoskeleton Organization

Having observed multiple tether and sling formation in Th1, Th17, and Treg cells, we hypothesized that a common gene signature might be induced in Th1, Th17, or Treg cells compared with Tn cells. Neutrophils form slings and were included in the analysis as a positive control. The Venn diagram shows the gene expression overlap among all sling-forming cells versus Tn cells (which do not form slings) (Figure 5A). We identified 347 transcripts uniquely enriched in Th1 cells, 257 in Th17 cells, and 146 in Treg cells. Remarkably, 4,177 transcripts (~33% of expressed transcriptome) were found to be significantly

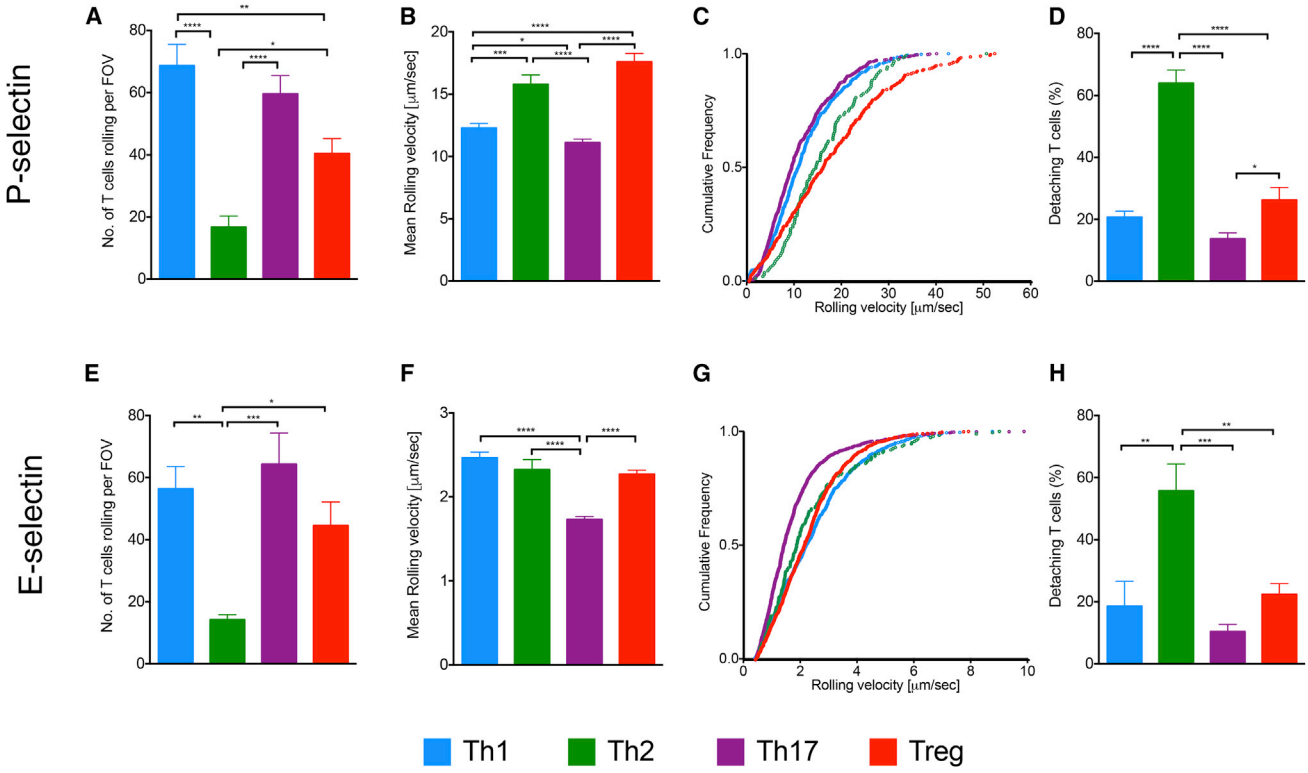

Figure 1. Rolling Behavior of Th1, Th2, Th17, and Treg Cells on P- and E-Eelectin-Fc

Mouse CD4 T cells were rolling on selectin-coated microfluidic flow chambers at 10 dyn/cm^2.

(A–D) Number (A), mean rolling velocities (B), cumulative histogram of rolling velocities (C), and percentage (D) of detaching T cells on P-selectin-Fc (2 μg/mL). Total number of rolling events was evaluated from at least eight independent movies per condition from three biological replicates. Rolling velocities were evaluated from 455 Th1, 120 Th2, 628 Th17, and 287 Treg cell tracks.

(E–H) Number (E), mean rolling velocities (F), cumulative histogram of rolling velocities (G), and percentage (H) of detaching T cells on E-selectin-Fc (2.5 μg/mL). Total number of rolling events was evaluated from at least six independent movies per condition from three biological replicates. Rolling velocities were evaluated from 516 Th1, 186 Th2, 1,090 Th17 and 727 Treg cell tracks.

The means for multiple comparisons were calculated using one-way ANOVA followed by the Kruskal-Wallis test. Data are mean ± SEM. *p < 0.05, **p < 0.01, ***p < 0.001, and ****p < 0.0001. FOV, field of view.

co-regulated in all sling-forming cells (Th1, Th17, and Treg cells and neutrophils) compared with Tn (Figures 5A and 5B).

To test for commonly activated pathways in Th1, Th17, and Treg cells during differentiation, we performed Ingenuity Pathway Analysis (IPA) using the 4,177 genes induced in all sling-forming cells. Each sling-forming cell type (Th1, Th17, and Treg cells or neutrophils) was compared with Tn cells separately, and then the intersection of 17 common predicted functional pathways was extracted (Figures 5C, 5D, and S7A–S7C). We found common functional pathways including cell movement, cellular infiltration, cell migration, cellular invasion, and organization of cytoskeleton. Interestingly, Th2 cells showed reduced activation of pathways related to cell migration (Figures 5D and S7D). Comparing the activation score of cell migration pathways among all T cell subsets revealed that genes related to organization of cytoskeleton may be important for tether and sling formation. We observed high Z scores in sling-forming cells and a low Z score in Th2 cells (Th1, Z = 2; Th17, Z = 2.1; Treg, Z = 2.7; Th2, Z = 0.2) (Figure 5E). Thus, all sling-forming cells undergo transcriptomic modifications that enhance cell migration pathways and cytoskeleton organization. In this list of genes (Table S2), we expect candidate genes encoding proteins required for tether and sling formation.

Human Th1 Cells Form Tethers and Slings

To test whether our findings in mice also apply to human T cells, we investigated tether and sling formation in human CD4 T cells. To this end, we isolated peripheral blood mononuclear cells (PBMCs) from blood of healthy donors and sorted the CD4 T cell subsets on the basis of their chemokine receptor expression (Gosselin et al., 2010; Acosta-Rodriguez et al., 2007). Live CD3$^+$CD4$^+$CD25$^-$ cells were further gated using CD45RA and CD45RO surface markers to differentiate between naive and memory T cell subsets, respectively. Within the memory T cell subset, Th1 cells were CXCR3$^+$CCR4$^-$CCR6$^-$, Th2 cells were CXCR3$^-$CCR4$^+$CCR6$^-$, and Th17 cells were CXCR3$^-$CCR4$^+$CCR6$^+$ (Figures 6A and S8A). Unlike mice from specific pathogen-free (SPF) facilities, free-living humans have significant numbers of Th1 cells in their blood (Farber et al., 2014). In our subjects, the number of Th2 and Th17 cells after

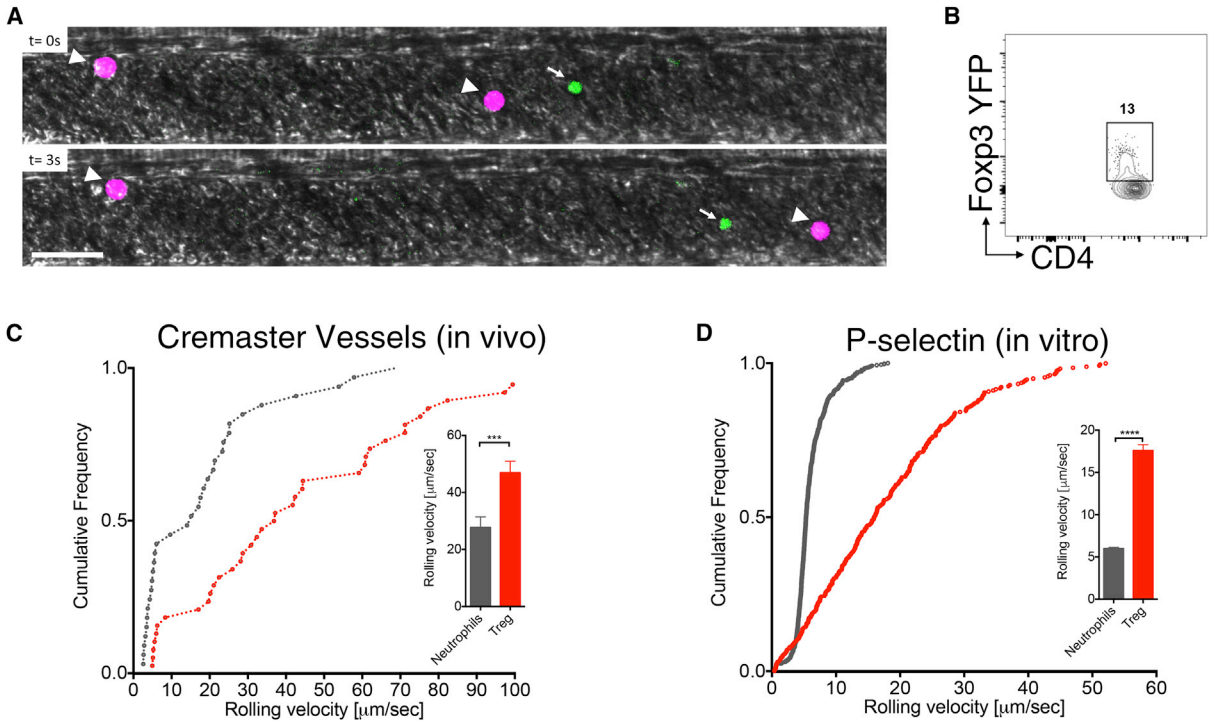

Figure 2. Rolling of Neutrophils and Treg Cells in Cremaster Venules *In Vivo*

(A) Representative images of neutrophils (Ly6G Alexa Fluor 647; arrowheads) or Treg cells (Foxp3 YFP; arrows) rolling in cremaster venule of Foxp3-YFP mouse. Blood flow direction is left to right. Scale bar is 30 μm. Contrast enhancement was done post-acquisition.

(B) Representative FACS plot showing the total percentage of CD4 Treg cells in blood of a Foxp3-YFP mouse.

(C and D) Cumulative histogram of neutrophil and Treg cell rolling velocities in cremaster postcapillary venules (*in vivo*) (C) and on P-selectin-Fc at 10 dyn/cm^2 (*in vitro*) (D). Inset: same data as bar graphs. Data in (C) are from n = 3 mice, n = 6 vessels (43 neutrophils and 49 Treg cells were analyzed). Average velocities in (D) are from more than three independent movies of three biological replicates (287 Treg cells and 606 neutrophils were tracked). Treg cell data are the same as in Figure 1B.

Data are mean ± SEM. The medians in (C) and (D) between two groups were calculated using the Mann-Whitney test. ***p < 0.001 and ****p < 0.0001. See also Movie S1.

sorting was too small to analyze functionally (Figure S8A). Th1 cells directly isolated from blood without *in vitro* culture expressed the Th1 signature marker IFN-γ as detected by flow cytometry and transcriptomics (Figures S8B and S8C). To compare expression levels of PSGL-1 glycosylation genes, we performed RNA-seq of human CD4 Tn and Th1 cells isolated from blood of four different donors (Table S1 and Figure S8E). The PCA blot segregated naive from Th1 cells in PC1 and PC2 (Figure S8F). The crucial genes for PSGL-1 glycosylation (*FUT7*, *FUT4*, and *GCNT1*) were elevated in Th1 compared with Tn cells (Figure S8D). In contrast to mouse cells, *TPST1* was high in human Tn cells.

To compare the rolling behavior of human Tn with Th1 cells, we allowed both cell types to roll on human P-selectin-Fc. Human Tn cells rolled at very high velocity (20 ± 1 μm/sec), even at very low shear stress (0.1 dyn/cm^2) (Figure 6B). Once shear stress was increased to 1 dyn/cm^2, all Tn cells detached and failed to roll (data not shown). On the other hand, human Th1 cells were able to roll efficiently at high shear stress (6 dyn/cm^2). Human Th1 cells rolled stably at low rolling speed (3 ± 0.4 μm/sec) (Figure 6B). In contrast to human Tn cells that did not form tethers and slings, Th1 cells formed about four or five tethers per cell (Figure 6C) and showed long slings, which reached up to ~30 μm (Figures 6D and 6E; Movie S4).

Next, we studied gene regulators and functional pathways in human Th1 cells. First, we compared and contrasted the differentially expressed genes in human and mouse Th1 versus Tn cells and found an overlap of 1,452 common genes (Figures 6F and 6H). The intersection of activated functional pathways in human or mouse Th1 showed genes that regulate cell movement, migration, homing, and cellular infiltration (Figures 6G and 6I). Thus, similar to mouse differentiated T cells, human effector cells are enriched in genes that regulate cell migration pathways, which likely induce alteration in cell morphology and enable sling formation.

DISCUSSION

We discovered a mechanism by which differentiated T cells roll and adhere to inflamed blood vessels at high shear stress by inducible tethers and slings. Selectin binding is required for most T cell rolling but is not sufficient for tether and sling formation. For example, naive CD4 T cells roll on the selectin ligand PNAd but are unable to form tethers or slings (Sundd et al.,

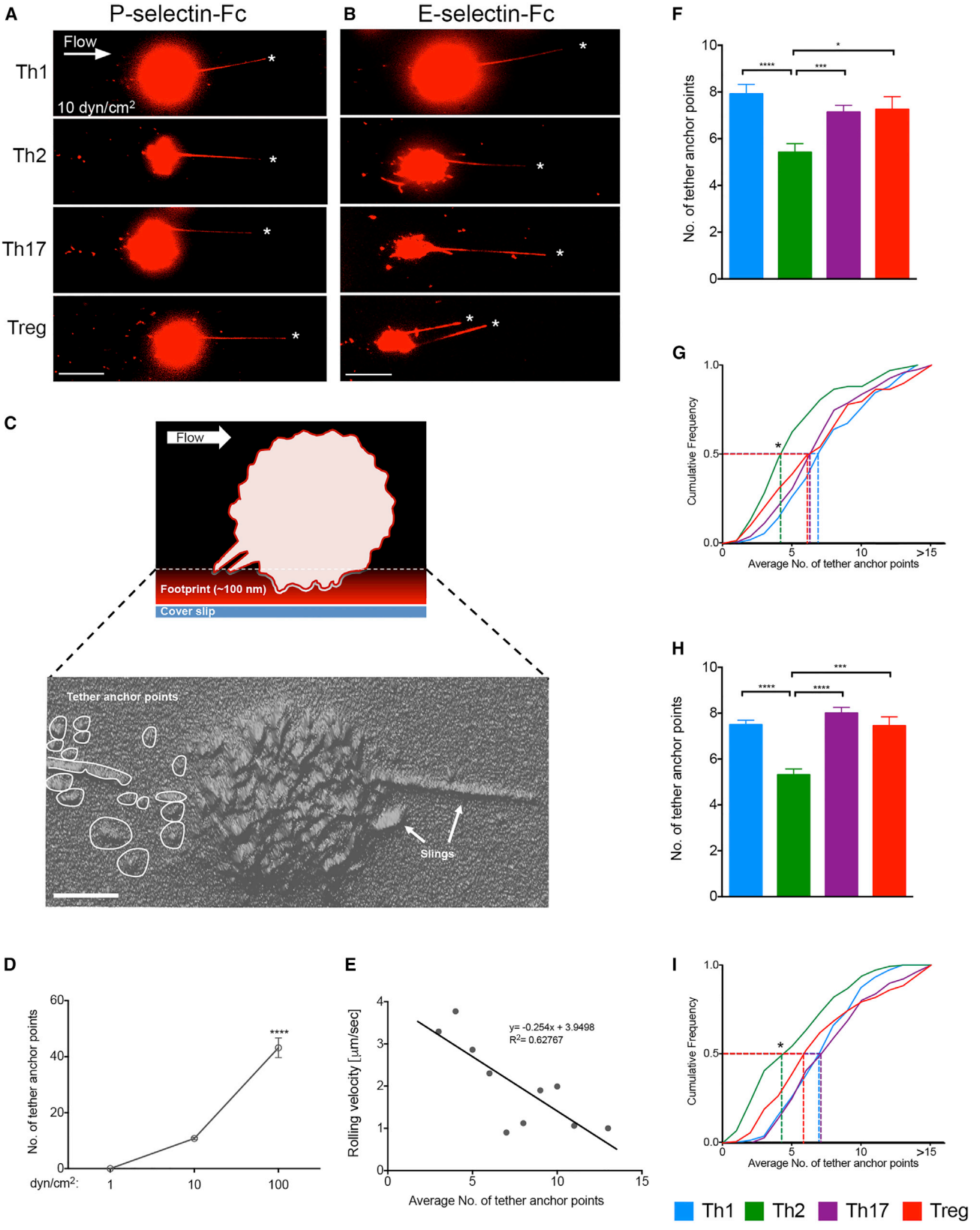

(legend on next page)

2012). Here, we discovered a transcriptomic program enabling tether and sling formation. Together, these allow stable rolling on selectins *in vitro* and *in vivo*. Also, we extended our findings to human blood Th1 cells.

In contrast to neutrophils that constitutively express functional PSGL-1, T cells modulate their PSGL-1 functionality in response to their activation state.

PSGL-1 functionality was previously studied in Th1 and Th2 cells (Atarashi et al., 2005; Bonder et al., 2006; Borges et al., 1997b). Here we extend these findings to Th17 and Treg cells, which had not been studied before. Although some studies reported higher PSGL-1 expression in Th1 cells than Th2 cells (Mangan et al., 2005; Xu et al., 2004), we confirm that Th1 and Th2 cells express similar levels of PSGL-1 protein (Bonder et al., 2005; Borges et al., 1997b). PSGL-1 surface expression was similar in all CD4 T cell subsets, but P-selectin binding was high in Th1, Th17, and Treg cells; significantly lower in Th2 cells; and absent in Tn cells. *In vitro* differentiation toward Th1 cells in the presence of IL-12 induces the transcriptional activation of STAT4, which boosts the levels of FucT-VII (*Fut7*) and C2GlcNAcT-I (*Gcnt1*) (Blander et al., 1999; White et al., 2001). Similarly, CD8 T cell activation by IL-12 induces P-selectin binding capacity (Carlow et al., 2001). However, we also observed *Fut7* and *Gcnt1* upregulated in Th17 and Treg cells, which are not induced by IL-12, suggesting that IL-12 is not required for the expression of these genes. This is consistent with a recent study showing that several other cytokines induce the expression of *Gcnt1* and *Fut7* transcripts (Ebel et al., 2015). We found even higher *Fut7* in Th17 and Treg cells than in Th1 cells. In contrast, *Gcnt1* and *Fut7* were not or only slightly upregulated in Th2 cells compared with Tn cells. This finding is consistent with the poor P-selectin binding by Th2 cells.

The highly functional selectin ligands in Th1, Th17, and Treg cells allowed a more stable rolling phenotype on P- and E-selectin compared with Th2 cells. Th1, but not Th2, cells were previously shown to successfully roll on P- or E-selectin *in vitro* at low shear stress (1–2 dyn/cm^2) (Atarashi et al., 2005; Bonder et al., 2006; Borges et al., 1997b). However, T cell rolling at high shear stress (6–10 dyn/cm^2), and tether and sling formation were not shown before. PSGL-1 is not required for tether and sling formation, because PSGL-1 knockout neutrophils still form tethers and slings on an E-selectin substrate (Sundd et al., 2012).

P-selectin binds both Th1 and Th2 cells, whereas E-selectin binds only to Th1 cells (Bonder et al., 2005). Here, we show that very few Th2 cells can roll on P- or E-selectin but at significantly higher velocity and higher detachment propensity than Th1 cells. PSGL-1 blockade partially inhibits Th1 cell migration *in vivo*, but blocking E-selectin had an additive effect (Bonder et al., 2005; Borges et al., 1997a; Hirata et al., 2000). On the basis of our findings, we predict that Th17 and Treg cells will also show P- and E-selectin-dependent homing to sites of inflammation. Like neutrophils (Zarbock et al., 2007), Th1, Th17, and Treg cells roll at significantly reduced velocities on E-selectin compared with P-selectin (note 6× different scale in Figures 1B and 1F). The rolling velocities of all cell types on P- or E-selectin were comparable, except for Th17 cells, which were the slowest. This may be related to the high expression of CD43, which supports Th17 rolling on E-selectin, whereas Th1 cells need the cooperation between CD43 and PSGL-1 to bind E-selectin (Velazquez et al., 2016). This can also explain the enhanced ability of Th17 cells to infiltrate lesion sites during atherosclerosis (Li and Ley, 2015) or CNS inflammation (Engelhardt and Ransohoff, 2012).

We also validated our findings *in vivo* by intravital imaging of endogenous Foxp3-YFP Treg cells in cremaster venules, which were able to roll stably at physiological shear stress. Treg rolling behavior *in vivo* was similar to our observations *in vitro*: in both cases, Treg cells roll well, almost as well as neutrophils. This is physiologically relevant, because Treg cell recruitment is important to maintain peripheral tolerance and keep inflammation under control. Treg cells home to sites of allograft pancreas transplantation (Zhang et al., 2009), but the mechanisms were not studied. We posit that they use tethers and slings to resist the high shear stress in such blood vessels. Endogenous Treg cells (Foxp3$^+$) that express high levels of *Fut7* and *Gcnt1* (van der Veeken et al., 2016) are the most suppressive (Miyara et al., 2015), suggesting that selectin binding is relevant for Treg cell recruitment.

Most Th1, Th17, and Treg cells that stably roll at 10 dyn/cm^2 form multiple tethers to resist this high shear stress. However, most Th2 cells detach because fewer of their microvilli are in

Figure 3. Differentiation Induces Tether and Sling Formation in CD4 T Cell Subsets

(A and B) Sling formation at 10 dyn/cm^2 in Th1, Th2, Th17, and Treg cells isolated from ROSA26mT/mG mice on (A) P-selectin-Fc (2 μg/mL) or (B) E-selectin-Fc (2.5 μg/mL). Scale bar is 10 μm. Asterisks denote the sling tips. Contrast enhancement was done post-acquisition to show slings. See also Movies S2 and S3.

(C) Schematic diagram shows the visibility of cell footprint by qDF (~100 nm). The cell membrane-localized tdTomato (red images in A and B) for one representative Treg cell rolling on E-selectin-Fc at 10 dyn/cm^2 was used to generate a 3D reconstruction of footprints to reveal slings, tether anchor points, and microvilli (hills) versus cell surface (valleys). White arrow shows the direction of rolling. Scale bar is 5 μm.

(D) Average number of tether anchor points per one representative Treg cell rolling at 1, 10, and 100 dyn/cm^2 on E-selectin-Fc. Data points are from at least six subsequent frames. The medians between two groups (10 versus 100 dyn/cm^2) were compared using the Mann-Whitney test. ****$p < 0.0001$.

(E) Correlation between mean rolling velocity at 10 dyn/cm^2 and number of tether anchor points per T cell. Data show ten different T cells (pool of Th1, Th2, Th17, and Treg cells) rolling at 10 dyn/cm^2 on P-selectin-Fc.

(F) Average number of tether anchor points per T cell rolling at 10 dyn/cm^2 on P-selectin-Fc. Total number of rolling events was evaluated from more than three independent movies per condition from three biological replicates (number of cells analyzed: Th1, n = 18; Th2, n = 12; Th17, n = 16; Treg, n = 15).

(G) Cumulative frequency of tether formation per T cell. Median indicated by dotted lines. Asterisk denotes median for Th2 cells.

(H) Average number of tether anchor points per T cell rolling at 10 dyn/cm^2 on E-selectin-Fc. Total number of rolling events was evaluated from more than three independent movies per condition from three biological replicates (number of cells analyzed: n = 10 for Th1, Th2, Th17, and Treg cells).

(I) Cumulative frequency of tether formation per T cell.

Median indicated by dotted lines. Asterisk denotes median for Th2 cells. The means in (F) and (G) for multiple comparisons were compared using one-way ANOVA followed by the Kruskal-Wallis test. Data are mean ± SEM. *$p < 0.05$, ***$p < 0.001$, and ****$p < 0.0001$.

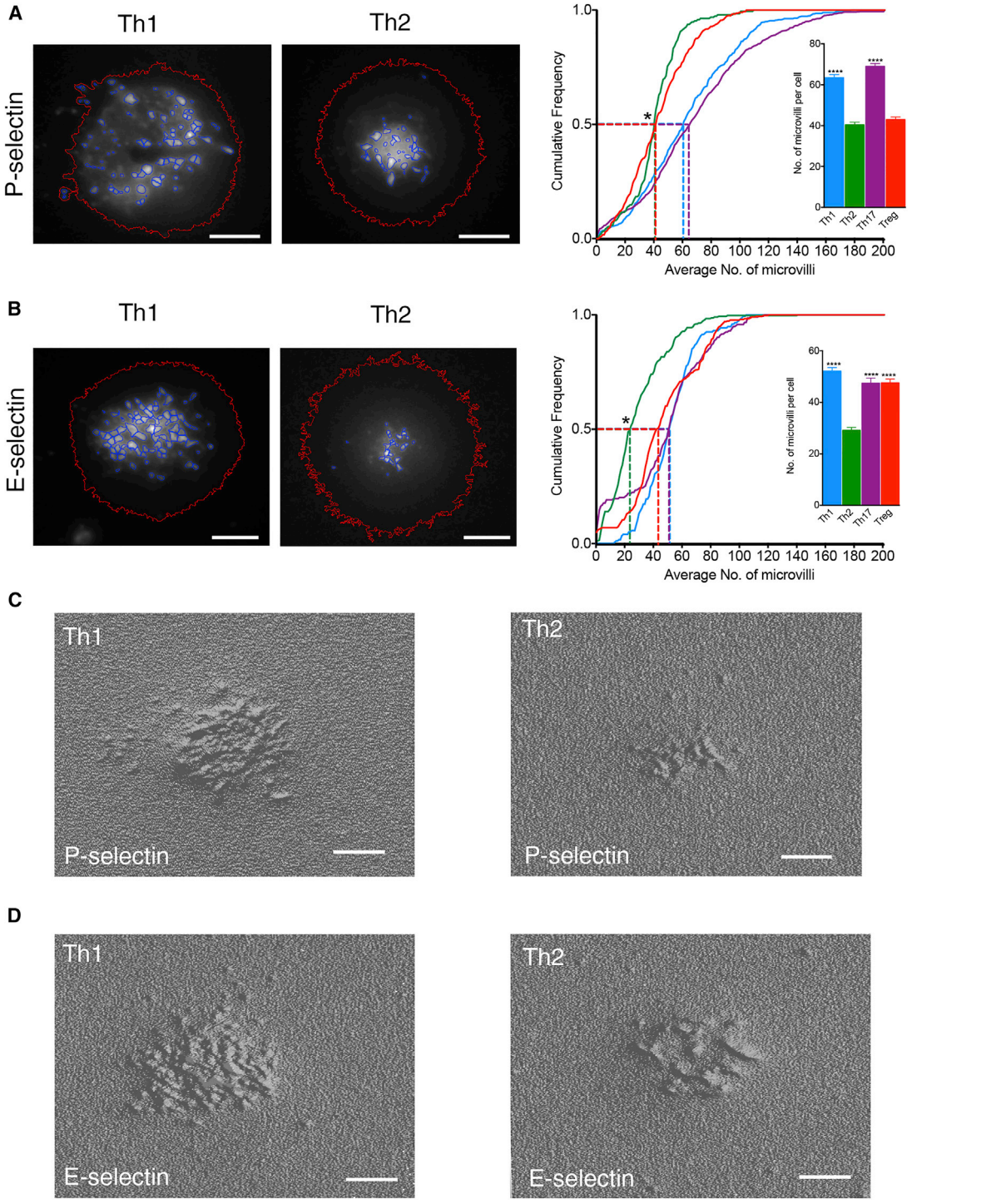

Figure 4. Numbers of Cell Footprint Microvilli Are Large in Th1, Th17, and Treg Cells

(A) Representative images of cell microvilli in Th1 and Th2 cells rolling on P-selectin-Fc at 10 dyn/cm^2 (left). Borders of cell microvilli are shown in blue. Borders of cell footprints are shown in red. Scale bar is 5 μm. Bar graph and cumulative histogram of average number of microvilli per cell in Th1, Th2, Th17, and Treg cells (right). Average number of microvilli was evaluated from more than three independent movies per condition from three biological replicates (number of cells analyzed: Th1, n = 56; Th2, n = 28; Th17, n = 126; Treg, n = 36). Median is indicated by dotted lines. Asterisk denotes median for Th2 cells.

(B) Representative images of cell microvilli in Th1 and Th2 cells rolling on E-selectin-Fc at 10 dyn/cm^2 (left). Borders of cell microvilli are shown in blue. Borders of cell footprints are shown in red. Scale bar is 5 μm. Bar graph and cumulative histogram of average number of microvilli per cell in Th1, Th2, Th17, and Treg cells

(legend continued on next page)

touch with the substrate, and tether formation is limited. These findings are consistent with the poor ability of Th2 cells, but not Th1 cells, to recruit into effector sites such as retinal parenchyma, skin, and lamina propria (Austrup et al., 1997; Haddad et al., 2003; Xu et al., 2004).

During T cell activation, transcriptional and epigenetic changes occur (Stubbington et al., 2015; Teague et al., 1999). Thus, the stimulation of Tn cells by cytokines will induce transcriptional reprogramming that controls the synthesis of a variety of molecules and enzymes required for cell morphology and motility. Tn cells lose their high surface expression of L-selectin upon T cell receptor (TCR) activation (Chao et al., 1997; Kaech et al., 2002) and gain glycosyl transferases that regulate surface glycan molecules (Comelli et al., 2006). Interestingly, all tether- and sling-forming cells showed similar transcriptomic regulation: they activate pathways related to cell motility, infiltration, and cytoskeletal organization. The role of cytoskeleton in tethers and slings is poorly understood. One recent study showed that the cytoskeletal regulatory proteins vasodilator-stimulated phosphoprotein (VASP) and Ena-VASP-like (EVL) are involved in effector, but not naive, T cell homing to inflamed sites (Estin et al., 2017). This suggests that cytoskeletal molecules might be involved in tether and sling formation.

Our finding that human Th1 cells induce tether and sling formation suggests that this could be clinically relevant. CD8 cytotoxic T cells, Th1 cells, and Th17 cells are now engineered to help eradicate tumors (Lim and June, 2017). Our work suggests that manipulating the transcriptome in chimeric antigen receptor (CAR) T cells could increase the efficacy of such treatments by boosting T cell homing to the tumor tissue. More work is needed to determine which genes are essential to provide high-efficiency rolling, tether formation, and recruitment.

Differentiated T cell trafficking to peripheral tissues is also critical for protective immunity from infectious organisms. Here we show that CD4 T cells not only acquire functional PSGL-1 upon differentiation but also undergo transcriptional changes that enable tethers to be pulled out from their surfaces. This inducible capability suggests that Th1, Th17, and Treg cells change their biomechanical properties during differentiation, allowing them to gain access to effector sites at high shear stress.

EXPERIMENTAL PROCEDURES

Mice

C57BL/6J mice (000664), ROSA26mT/mG mice (007676) (Muzumdar et al., 2007), and Foxp3 YFP reporter (016959) mice were obtained from The Jackson Laboratory (Bar Harbor, ME). Gender-matched mice (8–12 weeks old) were used in all experiments unless specified. All experiments followed guidelines of the La Jolla Institute for Allergy and Immunology Animal Care and Use Committee, and approval for use of mice was obtained from the La Jolla Institute for Allergy and Immunology according to criteria outlined in the Guide for the Care and Use of Laboratory Animals from the NIH.

In Vitro Mouse T Cell Polarization

Naive CD4 T cells were isolated from spleens of 8- to 12-week-old mice using the EasySep Mouse $CD4^+$ T Cell Isolation Kit (STEMCELL Technologies, Vancouver, Canada). Following isolation, purified CD4 T cells were differentiated *in vitro* in a 24-well plate coated with 8 μg/mL anti-mouse CD3ε (145-2C11) and 8 μg/mL anti-mouse CD28 (37.51) for 72 hr in the presence of 25 ng/mL recombinant mouse IL-12, 20 ng/mL recombinant mouse IL-2, and 1 μg/mL anti-mouse IL-4 (11B11) for Th1 differentiation; 50 ng/mL recombinant mouse IL-4, 20 ng/mL recombinant mouse IL-2, 1 μg/mL anti-mouse IL-12, and 1 μg/mL anti-mouse IFN-γ (XMG1.2) for Th2 differentiation; 50 ng/mL recombinant mouse IL-6, 5 ng/mL recombinant human TGF-β1, 1 μg/mL anti-mouse IL-4, and 1 μg/mL anti-mouse IFN-γ for Th17 differentiation; and 5 ng/mL recombinant human TGF-β1 and 20 ng/mL recombinant mouse IL-2 for Treg differentiation. Cytokines and antibodies were purchased from BioLegend (San Diego, CA).

Neutrophil Isolation and Phenotyping

Neutrophils were isolated from bone marrow of mice by cell sorting as described previously (Benarafa et al., 2011). Bone marrow cells were stained with anti-mouse surface markers PerCP-CD45 (30-F11), FITC-Ly6G (1A8), APC-CD115 (AFS98), PE-F4/80 (BM8), PE/Cy7-CD11c (N418), PE/Cy7-TER119, PE/Cy7-CD19 (6D5), eFluor 450-CD11b (M1/70), PE-CD4 (GK1.5), and PE-Siglec-F (E50-2440). Neutrophils were $CD45^+CD11c^+Ly6G^{hi}$, and promyelocytes were $CD45^+CD11c^+Ly6G^{lo}$. Promyelocytes were further distinguished from monocytes as $SSC^{hi}CD115^-$. Cell sorting was done using BD FACSAria II (BD Biosciences, San Diego, CA).

Human T Cell Isolation and Phenotyping

Human PBMCs were obtained from healthy donors through the LJI Clinical Core in accordance with the La Jolla Institute for Allergy and Immunology Normal Blood Donor Program (VD-057). PBMCs were isolated using SepMate tubes (STEMCELL Technologies). Then, PBMCs were stained by the anti-human surface markers Alexa Fluor 700 CD3 (UCHT1), eFluor 450 CD4 (OKT4), PE/Cy7-CD25 (BC96), PerCP-Cy5.5-CD45RA (HI100), Brilliant Violet 605-CD45RO (UCHL1), PE-CXCR3 (CEW33D), APC-CCR4 (D8SEE), and FITC-CCR6 (R6H1). The CD4 T cell subsets were sorted using BD FACSAria Fusion (BD Biosciences) on the basis of chemokine receptors expression (Acosta-Rodriguez et al., 2007; Gosselin et al., 2010). The visualization of high-dimensional single-cell data by viSNE was done using Cytobank software (Santa Clara, CA). For rolling assays, human Th1 cells were stained with 1 μg/mL cell mask deep red (Life Technologies, San Diego, CA) prior to imaging.

PSGL-1 Binding Assay by Flow Cytometry

CD4 T cells or neutrophils were incubated with 10 μg/mL recombinant mouse P-selectin-Fc for 30 min at room temperature (RT), followed by PE-anti-human-Fc secondary antibody and the surface markers FITC-CD4 (GK1.5), Alexa Fluor 700 TCR-β (H57-597), Alexa Fluor 647 CD162 (2PH1), or isotype control (RTK2071) for 30 min at RT. Neutrophils were stained with PerCP-CD45, FITC-Ly6G, and eFluor 450-CD11c. P-selectin binding to PSGL-1 was assessed by the total percentage of cells binding to the secondary anti-human-Fc antibody that exclusively binds the human-Fc part of recombinant mouse P-selectin. Data were acquired on a BD LSR II flow cytometer and FACSDiva software (BD Biosciences) and analyzed using FlowJo(OH, USA).

Intracellular Staining by Flow Cytometry

Cytokine production and transcription factor staining was done as described previously (Kimura et al., 2017). For cytoplasmic cytokine staining, cells

(right). Average number of microvilli was evaluated from more than three independent movies per condition from three biological replicates (number of cells analyzed: Th1, n = 13; Th2, n = 36; Th17, n = 22, Treg, n = 20). Median is indicated by dotted lines. Asterisk denotes median for Th2 cells.
(C) Footprints 3D reconstruction of representative Th1 (left) and Th2 (right) cells rolling on P-selectin-Fc at10 dyn/cm^2. Scale bars are 5 μm.
(D) Footprints 3D reconstruction of representative Th1 (left) and Th2 (right) cells rolling on E-selectin-Fc at10 dyn/cm^2. Scale bars are 5 μm.
The means in (A) and (B) for each cell type compared with Th2 were calculated using one-way ANOVA followed by the Kruskal-Wallis test. Data are mean ± SEM. ****$p < 0.0001$.

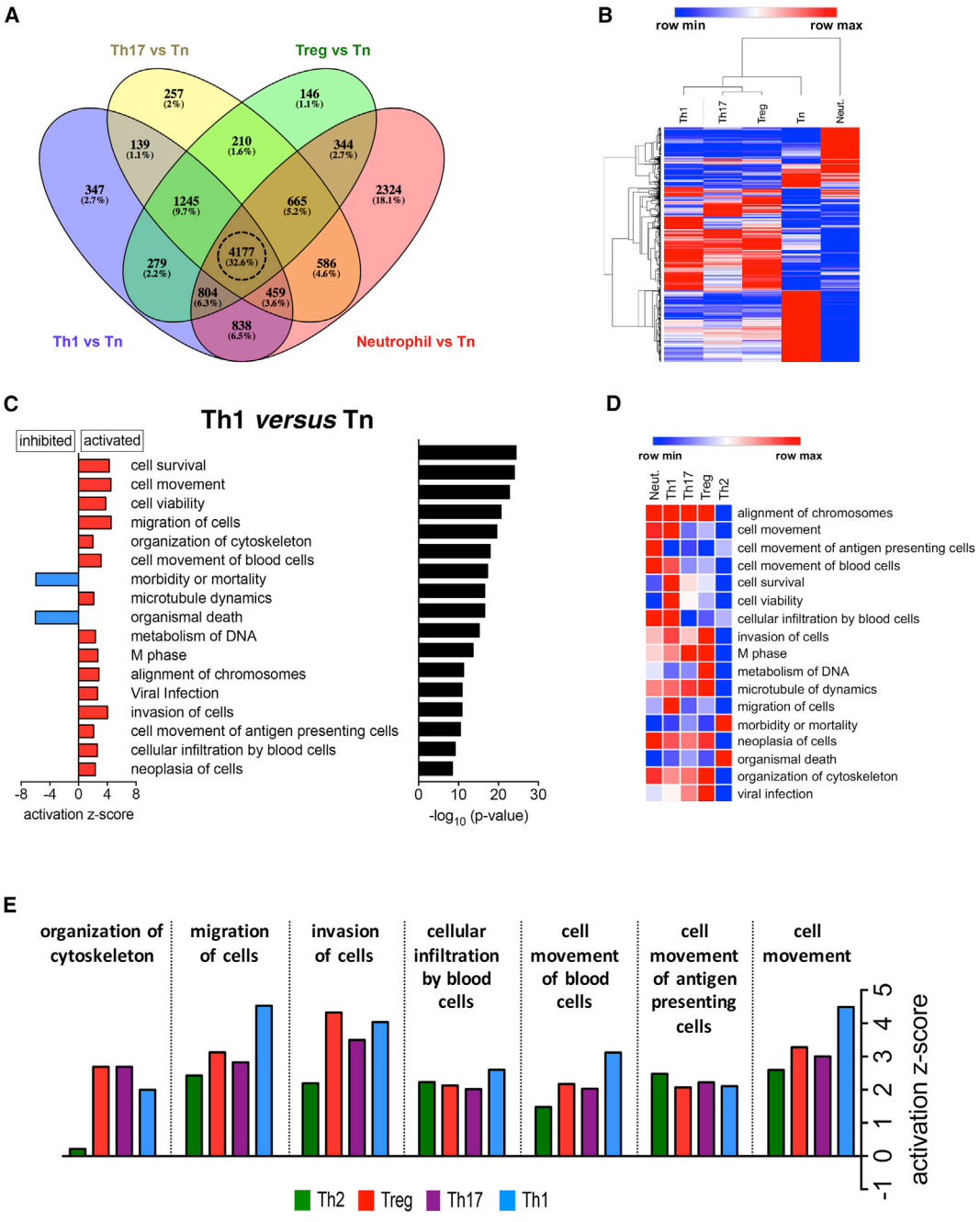

Figure 5. RNA-Seq Reveals Activation of Cell Migration-Related Genes in Sling-Forming Cells

(A) Venn diagram of differentially expressed genes between Th1 versus Tn, Th17 versus Tn, Treg versus Tn, and neutrophil versus Tn. Dotted circle shows the 4,177 common core genes.

(B) Hierarchically clustered heatmap (Pearson correlation) of the 4,177 common core genes shown in Venn diagram. Color bar scale shows row means. Red, high expression; blue, low expression.

(C) IPA of 4,177 genes reveals 17 common predicted functional pathways in sling-forming cells (Th1, Th17, and Treg cells and neutrophils) compared with Tn cells. The 17 common predicted activated and inhibited disease and functional pathways comparing Th1 versus Tn cells sorted by p value (cutoff <0.01) are shown. See also Figure S7 for Th17 versus Tn, Treg versus Tn, neutrophil versus Tn, and Th2 versus Tn comparisons. *Z* score reveals predicted activation (red bars) or inhibition (blue bars).

(D) Heatmap of predicted activated and inhibited disease and functional pathways between each comparison (Th1 versus Tn, Th17 versus Tn, Treg versus Tn, neutrophil versus Tn, and Th2 versus Tn) on the basis of p value (cutoff <0.01). Color bar scale shows row means. Red, high expression; blue, low expression.

(E) IPA of cell migration pathways shown in (D). *Z* score reveals predicted activation values.

See also Table S2 for organization of cytoskeleton genes list.

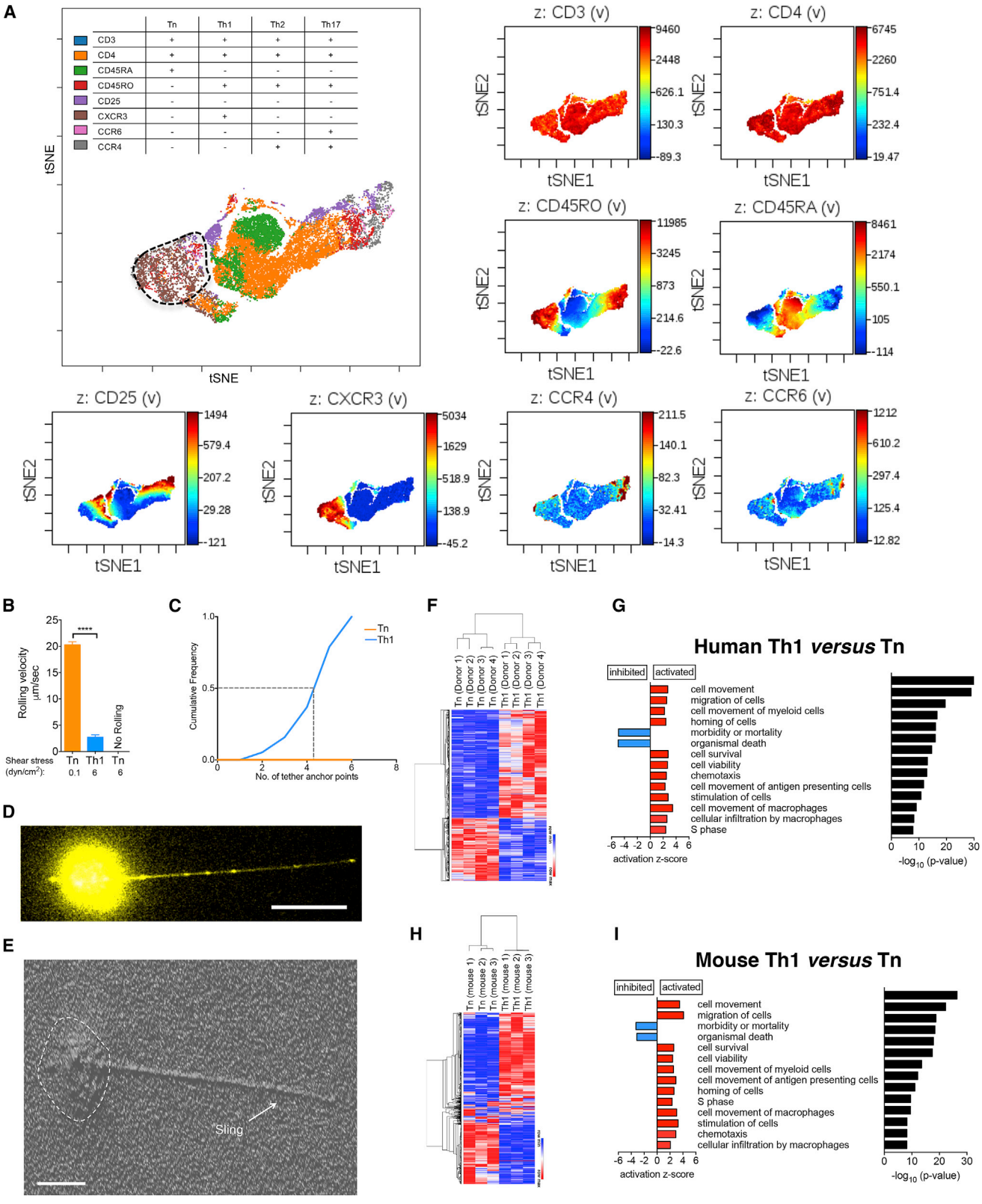

(legend on next page)

were stimulated with cell stimulation cocktail (eBioscience, San Diego, CA) with ionomycin and monensin for 5 hr at 37°C, fixed and permeabilized using Intracellular Fixation and Permeabilization Buffer Set (eBioscience), and stained with PE/Cy7-IL-17A (eBio17B7), Brilliant Violet 605 IFN-γ (XMG1.2), and PE-IL-4 (11B11) for 30 min at RT. For transcription factor staining, cells were fixed and permeabilized using FoxP3/Transcription Factor Staining Buffer Set (eBioscience) and stained with Alexa Fluor 488-Foxp3 (FJK-16 s) for 30 min at RT. For human samples, PBMCs were stained with PE/Cy7-IFN-γ (4SB.3), Brilliant Violet 605-IL-4 (MP4-25D2), and Brilliant Violet 711-IL-17A (BL168). Data were acquired on BD LSR II flow cytometer and FACSDiva software and analyzed using FlowJo.

In Vitro Live Cell Imaging

Sterile cover glass slides (24x60-1; Thermo Fisher Scientific) were coated with recombinant mouse P-selectin-Fc (2 μg/mL), recombinant mouse E-selectin-Fc (2.5 μg/mL), or recombinant human P-selectin-Fc (2 μg/mL) purchased from R&D Systems (Minneapolis, MN) for 2 hr at RT, followed by blocking with casein (Thermo Fisher Scientific, San Diego, CA) for 30 min. Ibidi sticky-Slides I 0.1 Luer (Ibidi, Martinsried, Germany) were mounted on the coated glass slides and connected with inlet and outlet tubing. T cells were then perfused through the inlet tube at a concentration of 1×10^6 cells/mL. The outlet tube was connected to a syringe pump (Harvard Apparatus). Wall shear stress was determined as descried previously (Abadier et al., 2015). First we allowed the cells to settle down for 1 min at 1 dyn/cm^2 for accumulation in the field of view and started imaging acquisition. The shear stress was then enhanced to 10 dyn/cm^2 for 2 min. To study the rolling behavior of T cells, image acquisition was performed at 10× magnification with an inverted Zeiss Axiovert 200M (Zeiss, Feldbach, Switzerland). The number of rolling cells was quantified during the 2 min acquisition after shear increase at 10 dyn/cm^2. The percentage of cell detachment was determined by counting the number of detached cells at 10 dyn/cm^2 as a fraction of total rolling cells during 2 min of acquisition. Mean rolling velocity was evaluated by tracking cells using IMARIS image analysis software or ImageJ software. To visualize tether anchor points and slings, acquisition was performed in a single-channel custom-made polydimethylsiloxane flow chamber using total internal reflection fluorescence microscopy (TIRFM) as described previously (Fan et al., 2016).

RNA Isolation and Sequencing

Tn, Th1, Th2, Th17, and Treg cells, neutrophils, and promyelocytes were phenotyped by flow cytometry as described above and sorted from three 8-week-old C57BL/6J female mice. Human Tn or Th1 cells were phenotyped and sorted from PBMCs isolated from four different donors (donor 1: female, 35 years; donor 2: female, 38 years; donor 3: male, 32 years; donor 4: female, 29 years). RNA was extracted from the sorted cells using Direct-zol RNA Kit (Zymo Research). RNA quality was determined using TapeStation Agilent 2200. The isolation of mRNA was done using the polyA method. RNA-seq was performed on the Illumina Hiseq 4000 following the SMARTseq II protocol from Illumina (San Diego, CA).

RNA-Seq Data Analysis

RNA-seq analysis was done as described previously (Li et al., 2016).

Cluster analyses including PCA and hierarchical clustering were performed using standard algorithms and metrics. Hierarchical clustering was performed using average linkage with Pearson correlation. Heatmaps were done using the Morpheus heatmap tool from the Broad Institute. The Venn diagram was created using Venny 2.1. DESeq2 (R package) was used to perform the differential expression analysis on the basis of the differences between the normalized gene counts between the groups (Love et al., 2014). We considered genes differentially expressed between two groups of samples when the DESeq2 analysis resulted in an adjusted p value of <0.01.

QIAGEN IPA

Differentially expressed gene lists were uploaded to IPA and processed using the Core Analysis function (Krämer et al., 2014). Disease and biological functions were used after negative log transformation of the p value overlap (cutoff $p < 0.01$). P value overlap and activation *Z* score were used to show significant activation or inhibition as a prediction of its effect on observed gene expression.

Footprint Quantification

Footprints of T cells isolated from ROSA26mT/mG mice were analyzed using CellProfiler (Kamentsky et al., 2011). Briefly, in each image, the total cell footprint was identified using an automatic threshold. The local background was subtracted, and then a second automatic threshold was used to segment the bright footprints, which show microvilli. Identified footprint regions were split into individual microvilli on the basis of intensity gradients, and the number of the microvilli (footprints) was found for each cell.

Three-Dimensional Reconstructions/Footprint Topography

Raw cell membrane-localized tdTomato (ROSA26mT/mG mice) image was used to create three-dimensional (3D) reconstructions (3D topography) by custom scripts in MATLAB (The MathWorks) as described previously (Fan et al., 2016).

Intravital Microscopy

To image Treg and neutrophil rolling *in vivo*, intravital microscopy of cremaster muscle venules from three 8-week-old Foxp3-YFP male mice was done. Mice were anesthetized throughout the experiment with isoflurane. To fluorescently label neutrophils, 2.5 μg of Alexa Fluor 647 anti-mouse Ly-6G antibody (clone 1A8) was retro-orbitally injected. The left cremaster muscle was exteriorized and prepared for imaging as described previously (Ley et al., 2008). Rolling

Figure 6. Tether and Sling Formation in Human Th1 Cells

(A) viSNE of PBMCs gated on live CD3$^+$CD4$^+$ events. Th1 cell subset is highlighted by dotted shape in expert gate. viSNE plots showing individual expression of surface markers. Red, high expression; blue, low expression.

(B) Mean rolling velocities of human Tn and Th1 cells on human P-selectin-Fc (2 μg/mL). Total number of rolling events was evaluated from at least three independent movies per condition from three biological replicates. Rolling velocities were evaluated from 7 Tn and 20 Th1 cell tracks. The means were compared using the unpaired t test. Data are mean ± SEM. ****$p < 0.0001$.

(C) Cumulative frequency of tether formation per human Th1 cell. Median is indicated by dotted lines.

(D) Sling formation in human Th1 cell rolling on P-selectin-Fc (2 μg/mL) at 6 dyn/cm^2. Yellow color denotes cell mask deep red labeling. Scale bar is 10 μm. Flow direction is left to right. Contrast enhancement was done post-acquisition to show the sling. See also Movie S4.

(E) 3D-reconstruction of cell footprints shown in (D). Scale bar is 5 μm. Comparing and contrasting "human Th1 versus Tn differentially expressed genes" and "mouse Th1 versus Tn differentially expressed genes" show 1,452 common core genes.

(F) Hierarchically clustered heatmap (Pearson correlation) of the 1,452 common core genes between human Th1 and Tn cells. Color bar scale shows row means. Red, high expression; blue, low expression.

(G) Predicted activated and inhibited disease and functional pathways comparing human Th1 and Tn cells sorted by p value (cutoff <0.01).

(H) Hierarchically clustered heatmap (Pearson correlation) of the 1,452 common core genes between mouse Th1 and Tn cells (same genes as in F). Color bar scale shows row means. Red, high expression; blue, low expression.

(I) Predicted activated and inhibited disease and functional pathways between mouse Th1 and Tn cells sorted by p value (cutoff <0.01). Color bar scale of heatmap shows row means. Red, high expression; blue, low expression.

See also Figure S8.

velocities of neutrophils or Treg cells were analyzed after manual tracking of individual cells using ImageJ software.

Statistics

Statistical analysis was performed using GraphPad Prism 6.0 (GraphPad Software, La Jolla, CA). The means for multiple comparisons were calculated using one-way ANOVA followed by the Tukey multiple-comparison test or non-parametric one-way ANOVA followed by the Kruskal-Wallis test. The means between two groups were calculated using the t test or Mann-Whitney test. Asterisks indicate significant differences (*$p < 0.05$, **$p < 0.01$, ***$p < 0.001$, and ****$p < 0.0001$).

DATA AND SOFTWARE AVAILABILITY

The accession number for the RNA-seq data reported in this paper is GEO: GSE107981.

SUPPLEMENTAL INFORMATION

Supplemental Information includes eight figures, four tables, and four movies and can be found with this article online at https://doi.org/10.1016/j.celrep.2017.11.099.

ACKNOWLEDGMENTS

We thank Jacqueline Miller from the La Jolla Institute for expert animal husbandry; Dr. Charaf Benarafa from the University of Bern, Switzerland, for expert help with developing the neutrophil sorting panel; Dr. Kristen Jepsen from IGM Genomics Center, University of California, San Diego (UCSD), for performing RNA-seq; Dr. Jason Greenbaum from the La Jolla Institute for mapping; Dr. Zbigniew Mikulski from the La Jolla Institute for microscopy technical assistance; and Cheryl Kim from the La Jolla Institute for flow cytometry technical assistance. This work was supported by grant R01HL078784 from the National Heart, Lung, and Blood Institute (NHLBI) to K.L. and fellowship P2BEP3-158972 from the Swiss National Science Foundation to M.A.

AUTHOR CONTRIBUTIONS

M.A. and K.L. designed experiments. M.A. performed most of the experiments and data analysis. A.B.P. performed RNA-seq mapping QC, DESeq2, and PCA plots. S.M. did the footprint analysis using CellProfiler. A.M. did the cremaster vessel imaging. Z.F. provided the MATLAB script. E.G. and A.G. designed the custom-made microfluidic device. M.A. and K.L. wrote the manuscript. K.L. supervised the project.

DECLARATION OF INTERESTS

The authors declare no competing interests.

Received: July 17, 2017
Revised: October 4, 2017
Accepted: November 28, 2017
Published: December 26, 2017

REFERENCES

Abadier, M., and Ley, K. (2017). P-selectin glycoprotein ligand-1 in T cells. Curr. Opin. Hematol. *24*, 265–273.

Abadier, M., Haghayegh Jahromi, N., Cardoso Alves, L., Boscacci, R., Vestweber, D., Barnum, S., Deutsch, U., Engelhardt, B., and Lyck, R. (2015). Cell surface levels of endothelial ICAM-1 influence the transcellular or paracellular T-cell diapedesis across the blood-brain barrier. Eur. J. Immunol. *45*, 1043–1058.

Acosta-Rodriguez, E.V., Rivino, L., Geginat, J., Jarrossay, D., Gattorno, M., Lanzavecchia, A., Sallusto, F., and Napolitani, G. (2007). Surface phenotype and antigenic specificity of human interleukin 17-producing T helper memory cells. Nat. Immunol. *8*, 639–646.

Atarashi, K., Hirata, T., Matsumoto, M., Kanemitsu, N., and Miyasaka, M. (2005). Rolling of Th1 cells via P-selectin glycoprotein ligand-1 stimulates LFA-1-mediated cell binding to ICAM-1. J. Immunol. *174*, 1424–1432.

Austrup, F., Vestweber, D., Borges, E., Löhning, M., Bräuer, R., Herz, U., Renz, H., Hallmann, R., Scheffold, A., Radbruch, A., and Hamann, A. (1997). P- and E-selectin mediate recruitment of T-helper-1 but not T-helper-2 cells into inflammed tissues. Nature *385*, 81–83.

Benarafa, C., LeCuyer, T.E., Baumann, M., Stolley, J.M., Cremona, T.P., and Remold-O'Donnell, E. (2011). SerpinB1 protects the mature neutrophil reserve in the bone marrow. J. Leukoc. Biol. *90*, 21–29.

Blander, J.M., Visintin, I., Janeway, C.A., Jr., and Medzhitov, R. (1999). Alpha(1,3)-fucosyltransferase VII and alpha(2,3)-sialyltransferase IV are up-regulated in activated CD4 T cells and maintained after their differentiation into Th1 and migration into inflammatory sites. J. Immunol. *163*, 3746–3752.

Bonder, C.S., Norman, M.U., Macrae, T., Mangan, P.R., Weaver, C.T., Bullard, D.C., McCafferty, D.M., and Kubes, P. (2005). P-selectin can support both Th1 and Th2 lymphocyte rolling in the intestinal microvasculature. Am. J. Pathol. *167*, 1647–1660.

Bonder, C.S., Clark, S.R., Norman, M.U., Johnson, P., and Kubes, P. (2006). Use of CD44 by CD4+ Th1 and Th2 lymphocytes to roll and adhere. Blood *107*, 4798–4806.

Borges, E., Pendl, G., Eytner, R., Steegmaier, M., Zöllner, O., and Vestweber, D. (1997a). The binding of T cell-expressed P-selectin glycoprotein ligand-1 to E- and P-selectin is differentially regulated. J. Biol. Chem. *272*, 28786–28792.

Borges, E., Tietz, W., Steegmaier, M., Moll, T., Hallmann, R., Hamann, A., and Vestweber, D. (1997b). P-selectin glycoprotein ligand-1 (PSGL-1) on T helper 1 but not on T helper 2 cells binds to P-selectin and supports migration into inflamed skin. J. Exp. Med. *185*, 573–578.

Carlow, D.A., Corbel, S.Y., Williams, M.J., and Ziltener, H.J. (2001). IL-2, -4, and -15 differentially regulate O-glycan branching and P-selectin ligand formation in activated CD8 T cells. J. Immunol. *167*, 6841–6848.

Chao, C.C., Jensen, R., and Dailey, M.O. (1997). Mechanisms of L-selectin regulation by activated T cells. J. Immunol. *159*, 1686–1694.

Comelli, E.M., Head, S.R., Gilmartin, T., Whisenant, T., Haslam, S.M., North, S.J., Wong, N.K., Kudo, T., Narimatsu, H., Esko, J.D., et al. (2006). A focused microarray approach to functional glycomics: transcriptional regulation of the glycome. Glycobiology *16*, 117–131.

Dixon, J.B., Greiner, S.T., Gashev, A.A., Cote, G.L., Moore, J.E., and Zawieja, D.C. (2006). Lymph flow, shear stress, and lymphocyte velocity in rat mesenteric prenodal lymphatics. Microcirculation *13*, 597–610.

Ebel, M.E., Awe, O., Kaplan, M.H., and Kansas, G.S. (2015). Diverse inflammatory cytokines induce selectin ligand expression on murine CD4 T cells via p38α MAPK. J. Immunol. *194*, 5781–5788.

Engelhardt, B., and Ransohoff, R.M. (2012). Capture, crawl, cross: the T cell code to breach the blood-brain barriers. Trends Immunol. *33*, 579–589.

Estin, M.L., Thompson, S.B., Traxinger, B., Fisher, M.H., Friedman, R.S., and Jacobelli, J. (2017). Ena/VASP proteins regulate activated T-cell trafficking by promoting diapedesis during transendothelial migration. Proc. Natl. Acad. Sci. U S A *114*, E2901–E2910.

Fan, Z., McArdle, S., Marki, A., Mikulski, Z., Gutierrez, E., Engelhardt, B., Deutsch, U., Ginsberg, M., Groisman, A., and Ley, K. (2016). Neutrophil recruitment limited by high-affinity bent β2 integrin binding ligand in cis. Nat. Commun. *7*, 12658.

Farber, D.L., Yudanin, N.A., and Restifo, N.P. (2014). Human memory T cells: generation, compartmentalization and homeostasis. Nat. Rev. Immunol. *14*, 24–35.

Fu, H., Ward, E.J., and Marelli-Berg, F.M. (2016). Mechanisms of T cell organotropism. Cell. Mol. Life Sci. *73*, 3009–3033.

Gosselin, A., Monteiro, P., Chomont, N., Diaz-Griffero, F., Said, E.A., Fonseca, S., Wacleche, V., El-Far, M., Boulassel, M.R., Routy, J.P., et al. (2010).

Peripheral blood CCR4+CCR6+ and CXCR3+CCR6+CD4+ T cells are highly permissive to HIV-1 infection. J. Immunol. *184*, 1604–1616.

Haddad, W., Cooper, C.J., Zhang, Z., Brown, J.B., Zhu, Y., Issekutz, A., Fuss, I., Lee, H.O., Kansas, G.S., and Barrett, T.A. (2003). P-selectin and P-selectin glycoprotein ligand 1 are major determinants for Th1 cell recruitment to nonlymphoid effector sites in the intestinal lamina propria. J. Exp. Med. *198*, 369–377.

Hirata, T., Merrill-Skoloff, G., Aab, M., Yang, J., Furie, B.C., and Furie, B. (2000). P-selectin glycoprotein ligand 1 (PSGL-1) is a physiological ligand for E-selectin in mediating T helper 1 lymphocyte migration. J. Exp. Med. *192*, 1669–1676.

Hobbs, S.J., and Nolz, J.C. (2017). Regulation of T cell trafficking by enzymatic synthesis of O-glycans. Front. Immunol. *8*, 600.

Kaech, S.M., Wherry, E.J., and Ahmed, R. (2002). Effector and memory T-cell differentiation: implications for vaccine development. Nat. Rev. Immunol. *2*, 251–262.

Kamentsky, L., Jones, T.R., Fraser, A., Bray, M.A., Logan, D.J., Madden, K.L., Ljosa, V., Rueden, C., Eliceiri, K.W., and Carpenter, A.E. (2011). Improved structure, function and compatibility for CellProfiler: modular high-throughput image analysis software. Bioinformatics *27*, 1179–1180.

Kimura, T., Tse, K., McArdle, S., Gerhardt, T., Miller, J., Mikulski, Z., Sidney, J., Sette, A., Wolf, D., and Ley, K. (2017). Atheroprotective vaccination with MHC-II-restricted ApoB peptides induces peritoneal IL-10-producing CD4 T cells. Am. J. Physiol. Heart. Circ. Physiol. *312*, H781–H790.

Krämer, A., Green, J., Pollard, J., Jr., and Tugendreich, S. (2014). Causal analysis approaches in Ingenuity Pathway Analysis. Bioinformatics *30*, 523–530.

Krummel, M.F., Bartumeus, F., and Gérard, A. (2016). T cell migration, search strategies and mechanisms. Nat. Rev. Immunol. *16*, 193–201.

Lawrence, M.B., Kansas, G.S., Kunkel, E.J., and Ley, K. (1997). Threshold levels of fluid shear promote leukocyte adhesion through selectins (CD62L,P,E). J. Cell Biol. *136*, 717–727.

Ley, K. (2014). The second touch hypothesis: T cell activation, homing and polarization. F1000Res. *3*, 37.

Ley, K., and Gaehtgens, P. (1991). Endothelial, not hemodynamic, differences are responsible for preferential leukocyte rolling in rat mesenteric venules. Circ. Res. *69*, 1034–1041.

Ley, K., and Kansas, G.S. (2004). Selectins in T-cell recruitment to non-lymphoid tissues and sites of inflammation. Nat. Rev. Immunol. *4*, 325–335.

Ley, K., Mestas, J., Pospieszalska, M.K., Sundd, P., Groisman, A., and Zarbock, A. (2008). Chapter 11. Intravital microscopic investigation of leukocyte interactions with the blood vessel wall. Methods Enzymol. *445*, 255–279.

Li, J., and Ley, K. (2015). Lymphocyte migration into atherosclerotic plaque. Arterioscler. Thromb. Vasc. Biol. *35*, 40–49.

Li, J., McArdle, S., Gholami, A., Kimura, T., Wolf, D., Gerhardt, T., Miller, J., Weber, C., and Ley, K. (2016). CCR5+T-bet+FoxP3+ effector CD4 T cells drive atherosclerosis. Circ. Res. *118*, 1540–1552.

Lim, W.A., and June, C.H. (2017). The principles of engineering immune cells to treat cancer. Cell *168*, 724–740.

Love, M.I., Huber, W., and Anders, S. (2014). Moderated estimation of fold change and dispersion for RNA-seq data with DESeq2. Genome Biol. *15*, 550.

Mangan, P.R., O'Quinn, D., Harrington, L., Bonder, C.S., Kubes, P., Kucik, D.F., Bullard, D.C., and Weaver, C.T. (2005). Both Th1 and Th2 cells require P-selectin glycoprotein ligand-1 for optimal rolling on inflamed endothelium. Am. J. Pathol. *167*, 1661–1675.

McEver, R.P. (2015). Selectins: initiators of leucocyte adhesion and signalling at the vascular wall. Cardiovasc. Res. *107*, 331–339.

McEver, R.P., and Cummings, R.D. (1997). Perspectives series: cell adhesion in vascular biology. Role of PSGL-1 binding to selectins in leukocyte recruitment. J. Clin. Invest. *100*, 485–491.

Miyara, M., Chader, D., Sage, E., Sugiyama, D., Nishikawa, H., Bouvry, D., Claër, L., Hingorani, R., Balderas, R., Rohrer, J., et al. (2015). Sialyl Lewis x (CD15s) identifies highly differentiated and most suppressive FOXP3high regulatory T cells in humans. Proc. Natl. Acad. Sci. U S A *112*, 7225–7230.

Muzumdar, M.D., Tasic, B., Miyamichi, K., Li, L., and Luo, L. (2007). A global double-fluorescent Cre reporter mouse. Genesis *45*, 593–605.

Perera, N.C., Wiesmüller, K.H., Larsen, M.T., Schacher, B., Eickholz, P., Borregaard, N., and Jenne, D.E. (2013). NSP4 is stored in azurophil granules and released by activated neutrophils as active endoprotease with restricted specificity. J. Immunol. *191*, 2700–2707.

Pickard, J.E., and Ley, K. (2009). Micro-PTV measurement of the fluid shear stress acting on adherent leukocytes in vivo. Biophys. J. *96*, 4249–4259.

Pospieszalska, M.K., Lasiecka, I., and Ley, K. (2011). Cell protrusions and tethers: a unified approach. Biophys. J. *100*, 1697–1707.

Ramachandran, V., Williams, M., Yago, T., Schmidtke, D.W., and McEver, R.P. (2004). Dynamic alterations of membrane tethers stabilize leukocyte rolling on P-selectin. Proc. Natl. Acad. Sci. U S A *101*, 13519–13524.

Sperandio, M., Gleissner, C.A., and Ley, K. (2009). Glycosylation in immune cell trafficking. Immunol. Rev. *230*, 97–113.

Stubbington, M.J., Mahata, B., Svensson, V., Deonarine, A., Nissen, J.K., Betz, A.G., and Teichmann, S.A. (2015). An atlas of mouse CD4(+) T cell transcriptomes. Biol. Direct *10*, 14.

Sundd, P., Gutierrez, E., Pospieszalska, M.K., Zhang, H., Groisman, A., and Ley, K. (2010). Quantitative dynamic footprinting microscopy reveals mechanisms of neutrophil rolling. Nat. Methods *7*, 821–824.

Sundd, P., Gutierrez, E., Koltsova, E.K., Kuwano, Y., Fukuda, S., Pospieszalska, M.K., Groisman, A., and Ley, K. (2012). 'Slings' enable neutrophil rolling at high shear. Nature *488*, 399–403.

Sundd, P., Pospieszalska, M.K., and Ley, K. (2013). Neutrophil rolling at high shear: flattening, catch bond behavior, tethers and slings. Mol. Immunol. *55*, 59–69.

Teague, T.K., Hildeman, D., Kedl, R.M., Mitchell, T., Rees, W., Schaefer, B.C., Bender, J., Kappler, J., and Marrack, P. (1999). Activation changes the spectrum but not the diversity of genes expressed by T cells. Proc. Natl. Acad. Sci. USA *96*, 12691–12696.

Theilgaard-Mönch, K., Jacobsen, L.C., Borup, R., Rasmussen, T., Bjerregaard, M.D., Nielsen, F.C., Cowland, J.B., and Borregaard, N. (2005). The transcriptional program of terminal granulocytic differentiation. Blood *105*, 1785–1796.

van der Veeken, J., Gonzalez, A.J., Cho, H., Arvey, A., Hemmers, S., Leslie, C.S., and Rudensky, A.Y. (2016). Memory of inflammation in regulatory T cells. Cell *166*, 977–990.

Velazquez, F., Grodecki-Pena, A., Knapp, A., Salvador, A.M., Nevers, T., Croce, K.J., and Alcaide, P. (2016). CD43 functions as an E-selectin ligand for Th17 cells in vitro and is required for rolling on the vascular endothelium and Th17 cell recruitment during inflammation in vivo. J. Immunol. *196*, 1305–1316.

von Andrian, U.H., and Mackay, C.R. (2000). T-cell function and migration. Two sides of the same coin. N. Engl. J. Med. *343*, 1020–1034.

White, S.J., Underhill, G.H., Kaplan, M.H., and Kansas, G.S. (2001). Cutting edge: differential requirements for Stat4 in expression of glycosyltransferases responsible for selectin ligand formation in Th1 cells. J. Immunol. *167*, 628–631.

Xu, H., Manivannan, A., Jiang, H.R., Liversidge, J., Sharp, P.F., Forrester, J.V., and Crane, I.J. (2004). Recruitment of IFN-gamma-producing (Th1-like) cells into the inflamed retina in vivo is preferentially regulated by P-selectin glycoprotein ligand 1:P/E-selectin interactions. J. Immunol. *172*, 3215–3224.

Zarbock, A., Lowell, C.A., and Ley, K. (2007). Spleen tyrosine kinase Syk is necessary for E-selectin-induced alpha(L)beta(2) integrin-mediated rolling on intercellular adhesion molecule-1. Immunity *26*, 773–783.

Zarbock, A., Ley, K., McEver, R.P., and Hidalgo, A. (2011). Leukocyte ligands for endothelial selectins: specialized glycoconjugates that mediate rolling and signaling under flow. Blood *118*, 6743–6751.

Zhang, N., Schröppel, B., Lal, G., Jakubzick, C., Mao, X., Chen, D., Yin, N., Jessberger, R., Ochando, J.C., Ding, Y., and Bromberg, J.S. (2009). Regulatory T cells sequentially migrate from inflamed tissues to draining lymph nodes to suppress the alloimmune response. Immunity *30*, 458–469.

Zhu, J., Yamane, H., and Paul, W.E. (2010). Differentiation of effector CD4 T cell populations (*). Annu. Rev. Immunol. *28*, 445–489.